Balloon-b measurements of stra ospheric and their precursors: implications for the production and loss of ozone

G. B. Osterman, R. J. Salawitch, B. Sen, R A Stachnik, I. M Pickett, G. C. Toon, J. J Margitan, J.- ' Blavier, and D. B. Peterson

Jet Propulsion aboratory/California nstitute of Technology, Pasadena

Abstract: Measurements of hydroge , nitrogen and chlorine radicals from a balloon flight on 25 September 1993 from Ft Sumner, NM provide an opportunity to quantify photochemical production and loss of ozone. Ozone loss rates determined using measured radical concentrations agree fairly well with rates calculated using a constrained photochemical model Catalytic cycles involving OH and IO_2 are shown to dominate photochemical loss of ozone loss for altitudes between 4ᴗ and 5ᴐ km Reactions involving NO and NO_2 are the dominant sink for ozone between 25 and 38 km. The total ozone loss rate determined from the measurements exceed production by ~35% above 42 km The sensitivity of the balance between production and loss of ozone to uncertainties in many of the controlling parameters is examined. The mbalance between production and loss is difficult to quantify, but none of the controlling parameters, taken individually, has a large enough uncertainty to result in excess productio of ozone in the upper stratosphere.

In roduction

The balloon flight on 25 September 993 from Ft Sumner, NM (34.5°N, 04.2°W) provided simultaneous measurements between 20 and 50 km altitude of the concentration of radicals NC ,

NO_2, C1O, I IO_2, and OI I. These species participate in catalytic cycles that arc the primary loss mechanism for stratospheric ozone. Measurements were also made of the concentration of longer lived species 0_3,1120, CH_4, N_2O_5, 1 INO_3, $ClNO_3$ and HCl that regulate the abundance of radicals. These measurements allow the balance between production and loss of stratospheric ozone to be quantified, and provide the first opportunity to examine simultaneously 10ss of ozone by hydrogen and chlorine radicals between 40 and 50 km.

Volume mixing ratio profiles of NO, NO_2, 0_3,1120, CH_4, N_2O_5, HNO_3, $ClNO_3$ and HCl were obtained using the Mkl V solar occultation interferometer, that typically obtains observat ions at sunrise and sunset [*Sen et al.*, this issue]. However, the high quality of tbc spectra acquired on ascent during this flight allowed retrieval of midday profiles for NO, NO_2 and 0_3. Concentrations of ClO, 1102 and O_3 were measured using the Submillimeter Limb Sounder (S1 ,S) [*Stachnik et al.*, in preparation]. 0_3 was also measured during the balloon ascent by an in sit u U J V photometer [*Margitan et al.*, in preparat ion]. Measurements of 011 were made using the Far Infrared Limb Observing Spectrometer (FILOS) [*Pickett and Peterson*, 1996].

Photochemical Model

The photochemical steady state model used here calculates the concentration of radical and reservoir species throughout a 24 hour period, for the latitude and temperature of the observations, with the requirement that the integral of production and 10ss of each species balances over a dail y cycle [*Salawitch et al.*, 1 994]. Balloon-borne measurements arc used to constrain the concentration of radical precursors such as 0_3, H_2O, CH_4, CO, C_2H_6, NO_y (defined to be NO -ı NO_2 -ı HNO_3 -ı $ClNO_3$ -ı 2×N_2O_5 -ı 1 INO_4 -ı I INO_2) and Cl_y (defined to be Cl -ı ClO

-1 HCl -1 $ClNO_3$ -1 HOCl -1 OClO + ClOO -1 2×Cl_2). The profile of aerosol surface area is obtained from zonal, monthly mean measuremen ts by the Stratospheric Aerosol and Gas Experiment (SAGE II) [*Yue et al.*, 1994]. The concentratio n of total inorganic bromine (Br_y) is specified from the correl at ion between brominated source gases and $N_2$0 [*Salawitch et al.*, 1994"1. Photolysis rates are calculated using a radiative transfer code that includes Rayleigh and aerosol scattering. Reaction rates and absorpt ion cross-sections are from *DeMore et al.* [1994]. React ion probabilities for sulfate aerosol heterogeneous reactions are: 0.1 for hydrolysis of N_2O_5, the formulation of *Hanson et al.* [1996] for the hydrolysis of $BrNO_3$, and the formulations of *Ravishankara and Hanson* [*1996]* for 1 ICI -1 $ClNO_3$, 110(:1-11 ICI> $ClNO_3$ -1 H_2O.

Model results presented here arc sensitive to the input ozone profile. Unless otherwise noted, the ozone profile used as input between O and 38 km is determined by averaging measurements obtained by Mkl V, Sl .S and an in situ UV photometer [*Margitan et al.*, in preparation]. Between 38 and 48 km, the S1 .S profile is used, and above 48 km a SAGE II profile close in location **(34.7°** N, 109,8" W) for the day previous to the balloon flight is used. The input ozone profiles and model sensitivity arc illustrated and discussed below.

Calculation of Ozone 1 ,0ss Rates

Measured concentratiomof011, 1102, ClO and NO_2 arc combined with theoretical concentrations of O and BrO to determine the removal rate of odd oxygen (Ox, defined to be the sum of the atomic oxygen and ozone concentrat ions) by each of the major radical families, The 24hour average concentration for 011, 1102, ClO and NO_2 is derived by fitting the diurnal profile calculated using the constrained photochemical model to the individual measurements,

which are available for limited portions of the day. The diurnal variation of each measured radical is obtained by scaling model curves at each altitude by a constant multiplicative factor, determined by least squares minimization of the residual between theory and observation,

1 Examples of the scaling process for observations obtained at 37 km are provided in Fig. 1. in general, tbc scaling factors are near unity, indicating the model closely matches the measured diurnal variation of each radical species. The model tends to overestimate 011 at 37 km by 20%, comparable to the 2σ measurement uncertainty. The diurnal variation of NO_2 at 37 km is simulated well by tbc mode]. The abundance of HO_2 is consistent with theory, although the measurement uncertainty at 37 km is larger than for the other radicals. Theory and observation are in close agreement for ClO, provided we allow for a 70/0 channel for production of 1 ICl from the reaction C10 + 011. The important.c of this or some other production mechanism for 1 ICl to the partitioning of chlorine species has been discussed extensively elsewhere [e.g., *Michelsen et* d., 1996].

The "empirical" rate for the reactions that limit loss of Ox is obtained by integrating, over 24 hours, the product of the scaled diurnal profiles for each reactant and the appropriate rate constant. Theoretical diurnal profiles for 0 and BrO are used since measurements of these gases are unavailable. The dominant Ox loss process by hydrogen radicals (I 10x) below ~30 km is limited by $HO_2 + O_3 \rightarrow OH + 2O_2$, while $HO_2 + O \rightarrow OH + O_2$ limits loss at higher altitudes. For chlorine radicals (C]x), the dominant cycle above -25 km is limited by $ClO + O \rightarrow Cl + O_2$, with the cycle limited by ClO + 1102-->1 IOCl + 0_2 making a secondary contribution. The only significant contribution to loss of O_x by nitrogen radicals (NO_x) is from the cycle limited by $NO_2 + O \rightarrow NO + 0_2$ [e.g., *Jucks et al.*, 1996].

Catalytic Cycle Contributions to Wont 1.0ss

Figure **2** illustrates the 24 hour average "empirical>' Ox loss rates for the HO_x, Cl_x and NO_x catalytic cycles. 1 'rror bars in Fig. 2 represent a root-sum-of-the-squares combination of the 10 precision uncertainties of the individual radical measurements, the uncertainties in the rate of the limiting, reactions from *DeMore et al.* [1 994], and a 20% uncertainly in the concentration of O primarily due to the photolysis rate of 0_3. The figure also contains profiles of O_x 10ss rates for each radical family calculated using the photochemical model, constrained by the balloon measurements of radical precursors.

Figure 2 illustrates the dominance of the NO_x contribution to O_x loss in the 25 to 38 km region, as expected from theory. The empiric.al and theoretical profiles for the NO_x contribution agree to within 2 to 10°/0 for altitudes between 30 and 38 km. The model underestimates tbc NO_x contribution to O_x loss by 30 to **60°/0** below 24 km. This discrepancy is caused by the tendency of observed NO_2 at sunset to exceed theoretical estimates below 26 km, and is related to difficulties in simulating the NO_2/NO ratio [*Sen et al.*, 1996]. It is unclear how resolution of this discrepancy will affect O_x loss rates in the lower stratosphere.

The agreement between empirical and model rates for the Cl_x contribution shown in Fig. 2 is typically within 1 O%, provided wc assume a 7% channel for production of 1 ICl from C](H011. If wc assume no production of 1 ICl from ClO+011, the model overestimates the Cl_x contribution by a factor of 1.5 to 2.0 between 25 and 45 km. *Jucks et al.* [1996] reached similar conclusions based on observations that extended to 38 km.

The S1 .S mcasurcmcntsof1102 demonstrate that 1 IO_x is the dominant contributor to 10ss of O_x above 45 km, in agreement with theory (1 'ig. 2). 1 lowever, the model consistently

underestimates the HO_x contribution to O_x loss between 40 and 50 km, with the largest discrepancy at 42 km (38%), and better agreement above 45 km (differences <19%). Between 30 and 40 km, the accuracy of the SLS measurements of 1102 is not as good as the FILOS measurements of011. Consequently, wc have obtained a second estimate for the HO_x contribution to 10ss of O_x based on FILOS OH and the model value of the OH/HO_2 ratio. The error bars in Fig. 2 for the FILOS OH based estimate of O_x 1oss arc dominated at all altitudes by uncertainty in the rate of HO_2+O, while those for the S1 .S HO_2 estimate arc dominated by uncertaint y in this rate for alt itudes above 40 km and by uncertaint y in the measurement of HO_2 below 35 km.

The agreement between the two profiles for loss of O_x due to HO_x is reasonabl y good, varying between 5 and 29°/0. The theoretical profile for the HO_x contribution agrees with the two empirical HO_x rates to within 5 to 35°/0, with the model value typically located between the two empirical rates.

Another kcy contributor to loss of O_x is recombination of odd oxygen ($O+O_3$). Since measurements of atomic oxygen arc not available for this flight, only the mode] profile for the rate of $O+O_3$ is included in Fig. 2. The contribution of $O+O_3$ exceeds 10°/0 at altitudes above 35 km. The contribution to the loss of O_x from reactions involving BrO (not shown) is ~20% at 20 km and declines rapidly with increasing altitude.

Ozone Production and Loss

There have been many studies of the imbalance between production and loss of ozone, often referred to as the "ozone deficit" problem. Generally it has been determined that ozone 1oss

exceeds production by 10 to 500/0 in the upper stratosphere. Production and loss of O_x arc expected to balance for altitudes above 30 km at mid-latitudes since the photochemical lifetime of O_x is short compared to the time constant its redistribution by transport [e. g., *Minschwaner et al.*, 1993 and references therein].

"1 Empirical" total O_x 10ss rates derived from the radical measurements (1_{EMP}) arc plotted in Fig. 2 as solid triangles between 30 and 38 km, wheremeasurcmcntsof011, 1 IO_2, ClO and NO_2 arc available, and as unfilled triangles between 40 and 50 km to indicate where measurements of NO_2 arc unavailable and theoretical values for the contribution to loss of O_x from NO_x arc used for determination of 1_{EMP}. Between 30 and 40 km, the HO_x contribution to 1_{EMP} is obtained by averaging rates inferred from S1 .S HO_2 and FH.OS OH. Model values for contributions from OHO_3 and reactions involving BrO arc used for all altitudes, Profiles for the total O_x loss rate (all catalytic cycles) calculated using the constrained photochemical model (1_{MODEL}) and the production rate Of O_x from photol ysis of O_2 (P_{MODEL}) arc also shown in Fig. 2. The 1σ uncertainty in P_{MODEL} is ~20% at all altitudes [e.g., *Minschwaner et al.*, 1993]. An a priori estimate. of the uncertainty in 1_{MODEL} is difficult to obtain since it involves numerous kinetic, photolytic and atmospheric (i.e., radical precursor) terms, not to mention possible unaccounted for processes (i.e., ClO + 1102-->1 $ClHO_3$).

The empirically determined O_x 10ss rate (1_{EMP}) agrees with the theoretical profile (1_{MODEL}) to within 1 00/0 over the entire altitude range, suggesting photochemical removal Of stratospheric 0_3 by known processes involving the measured radical species occurs at a rate close to the theoretical value. For altitudes at or below 40 km, $1,1_{MP}$ agrees with P_{MODEL} to within the uncertainties of the radical measurements and the rates of the limiting reactions, suggesting that

production and loss of O_3 are close to being balanced. This result is in agreement with earlier studies using balloon [*Jucks et al., 1996*] and ATMOS data [*Minschwaner et al., 1993*].

For altitudes above 42 km, L_{TEMP} exceeds P_{MODEL} by ~35%, suggesting the existence of a sizable O_3 deficit. The uncertainties in our determinations of L_{TEMP} and P_{MODEL} suggest the deficit could range from -15 to 60% between 42 to 50 km. The uncertainty in L_{TEMP} at 50 km is 34%, with the largest contributions from the rate of HO_2+O (26%), and concentrations of atomic oxygen (20%) and HO_2 (10%).

The sensitivity of O_x loss to uncertainties in the profile of O_3 must be examined to reach realistic conclusions regarding the implications of the balloon data. *Dessler et al.* [1996] showed the calculated ozone deficit could be reduced or even change sign (i.e., an ozone surplus) depending on the O_3 profile. The sensitivity of L_{MODEL} to the input O_3 profile is illustrated in Fig. 3. The profile used below 38 km is based on the balloon-borne measurements, as described previously, while above this height, three profiles are used: Halogen Occultation Experiment (HALOE) [J. *M. Russell*, private communication] (33.6° N, 109.8° W, dashed line, 38 to 60 km), SAGE/SAGE II (solid line, identical to that described earlier) and Microwave Limb Sounder (MLS)/SAGE II [*L. Froidevaux*, private communication] (35.5° N, 109.6° W, dotted line, MLS from 38-48 *km*). The latitude of the data from HALOE, SAGE II and MLS were matched as closely as possible to that of the balloon flight, and were within a day of the flight.

The model was used to determine O_x loss rates for each O_3 profile in Fig. 3a, with results plotted in Fig. 3b. Only one curve for production is shown since variations in P_{MODEL} are minimal for the three Mont profiles. The differences in the ozone profiles yield significant variations in L_{MODEL}. This behavior results primarily from an enhancement in the concentration

of atomic oxygen proportional to the increase in ozone, leading to an increase in the efficiency of each significant catalytic cycle above 38 km. This process is illustrated in Fig. 3a and 3b: as the input O_3 profile increases for altitudes between 42 and 50 km, the associated values of L_{MODEL} rise accordingly. Since L_{TEMP} will respond to variations in the profile of O_3 in a manner similar to L_{MODEL}, results for L_{MODEL} in Fig. 3b may be viewed as a surrogate for the sensitivity of the empirical loss rates. The imbalance between production and loss of O_x above 50 km, where radical measurements are unavailable, is markedly reduced if the actual O_3 profile were as low as the HALOE measurement. Nonetheless, an O_3 deficit exists at all altitudes. Unless the true O_3 profile was significantly lower than the HALOE profile, our results indicate it is unlikely that an ozone surplus existed above 45 km for the *DeMore et al.* [1994] rates and cress sections, such as reported by *Crutzen et al.* [1995] in their model study using HALOE and MLS ClO.

Several mechanisms have been proposed to alleviate the ozone deficit, either by decreasing the ozone loss rate or by increasing the production rate. Fig. 3c-e illustrate P_{MODEL} and L_{MODEL} calculated assuming different rates for certain key reactions. The SBUV/SAGE O_3 profile is used, and except for specific reactions of interest, all rates are from *DeMore* et *al.* [1994]. Also included in Fig. 3c-e are profiles for L_{TEMP} corresponding to each calculation.

Figure 3c contains two profiles of L_{MODEL} for 0% yield (solid lines) and 7% yield (dashed lines) of HCl from ClO+OH. As discussed previously, L_{MODEL} agrees more closely with L_{TEMP} (based on measured ClO) and P_{MODEL}, for altitudes between 35 and 40 km, when the 7% channel is assumed. Above 45 km, the importance of the Cl_x contribution to O_x loss decreases, and the 7% loss profile becomes indistinguishable from the 0% profile.

Figure 3d illustrates the effect on 1_{EMP} and I_{MODEL} Of a 19% increase in the rate Of $O + O_2 + M \rightarrow O_3 + M$, as suggested by *Eluszkiewicz and Allen [1993].* increasing this rate lowers atomic O, decreasing the rate Of each limiting reactions. Figure 3d shows this change in the rate of $O + O_2 + M$ brings production and loss of O_x into better agreement, but does not completely eliminate the deficit above 40 km.

Another possibility for resolution of the ozone deficit, especially above 50 km, is to decrease the effectiveness of the HO_x cycle [*Eluszkiewicz and Allen, 1993]. Summers et al.*[1996] concluded that models tend to overestimate, by roughly 40 to 50°/0, the amount of011 compared to measurements by the Middle Atmosphere Spectrograph Investigation (MA} 11<S1) between 5(I and 65 km. They showed a 50 to 70°/0 decrease in the rate of 1102-10- >011+ O_2 improved agreement bet ween model and measured OH. Figure 3e shows values for O_x production ant] 10ss for a 50% decrease in the rate of 1 IO-I O. The imbalance between I_{MODEL} and P_{MODEL} is greatly reduced at all altitudes, However, compared to the other cases in Fig. 3, there is a much larger discrepancy between I_{MODEL} and I_{EMP}. This discrepancy is the result of the model underestimating the observed concentrations of OH and HO_2, leading to lower O_x loss rates from the HO_x cycles. Clearly, themcasurcmcntsof011 and 1 HO_2 here disagree with those of MA I IRSI. Consequently, it is unlike] y that such a large change to the rate of $HO_2 + O$ is the key to resolving the imbalance between ozone production and loss.

Model calculations show that the altitude profile of the quantity $J_{O3}f_{O3}$, (where J_{O3} is the 24 hour average photolysis rate Of O_3 and f_{O3} is the ozone mixing ratio) is similar in shape to the profile Of the difference between 1_{MODEL} and P_{MODEL}, up to 50 km. This suggests production Of

OX from vibrationally excited O_2 could account for the imbalance between L_{MODEL} and P_{MODEL}, as discussed in greater detail by *Minschwaner et al.* [1993].

The analysis presented here suggests photochemical removal of ozone exceeds production for altitudes above 40 km for the rates and cross sections of *DeMore et al.* [1994], with the imbalance growing with increasing altitude. It is difficult to quantify precisely the magnitude of the "ozone deficit" in the upper stratosphere due to uncertainties in key parameters such as the rates of $O(^1D) + O_2 + M$, photolysis of O_2 and O_3, and the concentration of O_3. However, none of these parameters taken individually has a large enough uncertainty to result in excess ozone production. Further refinement of these parameters, as well as measurement of the concentration of atomic O, will be necessary to better quantify the imbalance between production and loss of ozone.

Acknowledgements. This research was performed at Jet Propulsion Laboratory, California Institute of Technology, under contract with the National Aeronautics and Space Administration.

References

Crutzen, 1'. J., J.-U. Grooß, C. Bruhl, R. Muller, and J. M. Russell, 111, A reevaluation of the ozone budget with 1 I Al /OE UARS data: No evidence for the ozone deficit, *Science*, 268, **705-708, 1995.**

I DeMore, W. B. et al., Chemical kinetics and photochemical data for usc in stratospheric modeling -1 Evaluation number 11, JPL, l'abdication 94-26, 1994.

1 Dessler, A. 1 E. et al., UARS measurements of ClO and NO_2 at 40 and 46 km and implications for the model "ozone deficit", *Geophys. Res. Lett.*, 23, 339-342, 1996.

Eluszkiewicz, J. and M. Allen, A global analysis of the ozone deficit in the upper strat osphere and lower mesosphere, *J. Geophys. Res., 98*, 1069-1082, 1993,

1 Ianson, 1). R., A. R. Ravishankara anti E.R. Lovejoy, Reactions of $BrONO_2$ with H_2O on submicron sulfuric acid aerosol and the implications for the lowest stratosphere, *J. Geophys. Res., 101*, 9063-9069, 1996.

Jucks, K. W. et al., Ozone production and loss rate measurements in the middle st rat osphere, *J. Geophys. Res., in press*, 1996.

Michelsen, 11. A. et al., Stratospheric chlorine partitioning: Constraints from shuttle-borne measurements of [HCl], [$ClNO_3$], and [ClO], *Geophys. Res. Lett*, 232361-2364, 1996.

Minschwaner, K., R. J. Salawitch, and M. B. McElroy, Absorption of solar radiation by O_2: Implications for O_3 and lifetimes of N_2O, $CFCl_3$, and CF_2Cl_2, *J. Geophys. Res., 98*, 10,543-10,561, 1993.

Pickett, 11. M. and D. B. Peterson, Comparison of measured stratospheric OH with prediction, *J. Geophys. Res., 101*, 16,789-16,796, 1996,

Ravishankara, A. R. and 1). R. 1 lanson, 1 Differences in the reactivity of type.- 1 polar stratospheric clouds depending on their phase, *J. Geophys. Res., 101*, 3885-3890, 1996.

Salawitch, R, J. et al., The distribution of hydrogen, nitrogen, and chlorine radicals in the lower stratosphere: Implications for changes in O_3 due to emission of NO_y from supersonic aircraft, *Geophys. Res. Lett., 21*, 2547-2550, 1994.

Summers, M. E. et al., Mesospheric HO_x photochemistry: Constraints from recent sate] 1 itc measurements, *Geophys. Res. Lett.*, 23, 2097-2100, 1996,

Yue, G. K., L. R. Poole, P. -11. Wang, and E. W. Chiou, Stratospheric aerosol acidity, density and refractive index deduced from SAGE 11 and NMC temperature data, *J. Geophys. Res.*, 99, 3727-3738, 1994.

G.B. Osterman, R.J. Salawitch, B. Sen, R. A. Stachnik, H.M. Pickett, G.C. Toon, and J.J. Margitan, Jet Propulsion Laboratory, (California Institute of Technology, M.S. 183-301, 4800 Oak Grove 1 hive, Pasadena, CA, 91109. (c-mail: gbo@caesar.jpl.nasa.gov)

Figure 1. Diurnal profiles of011 (FILOS), 1 IO_2 (S1 .S), NO_2 (Mkl V) and ClO (S1 .S) at ~37 km. The squares are the data for each species, the solid black curve represents the model calculated profile for each radical species and the dotted curve is the least squares fit Of the model profile to the data. The balloon ascent was in the afternoon of 25 September 1993, reached a float altitude of ~38 km. The balloon floated all night and descent took place on the morning of the 26th (approximately 0900 I .T).

Figure 2. The ozone 10ss rates vs. altitude for each catalytic cycle. 1 :mpirical results are contributions from: HO_x calculated using S1 .S HO_2 (open red circles), HO_x determined from FILOS OH and the model OI 1/1 IO_2 ratio (filled red circles), Cl_x obtained from S1 .S ClO (green squares), NO_x determined from Mkl V NO_2 (blue diamonds). The total empirical OX loss rates $1_{.EMP}$ are plotted as: filled triangles corresponding to total rate calculated using all measured radical cycles and open triangles using the model calculated NO_x contributions above 38 km. Model values arc shown for contributions from: $O+O_3$ (purple dash-dot line), NO_x (blue dotted line), Cl_x (green dashed line), HO_x (red dash-dot line), as WC]] as total O_x loss rate $1_{.MODEL}$ (solid black line) and O_x production P_{MODEL} (black dash-dot line).

Figure 3: I'ant] (a) three ozone profiles input to the model to test the sensitivity of tbc ozone deficit (see text for details). Panel (b) shows tbc variation in the model calculated O_x loss rate ($L_{.MODEL}$) profiles corresponding to the different ozone inputs. Panel (c) shows the calculated P_{MODEL} (dash dot dot) and $L_{.MODEL}$ (solid) for the SI.S/SAGE II ozone input assuming all reaction rates in the model arc given by JPI. 94 recommended rates and a second calculation of $L_{.MODEL}$ assuming a 70/0 yield Of 1 ICl from ClO+011 (dashed). The values of $L_{.EMP}$, calculated for Fig. 2 arc also shown (triangles). Pane] (d) is the same as (c) except that the only deviation from the JPI. 94 rates is a 19% increase in the rate of $O_{1}02\text{-}1 M \rightarrow O_3 + M$. Panel (c) is similar to (c.) except tbc reaction $HO_2 + O \rightarrow OH + O_2$ is decreased by 50°/0.

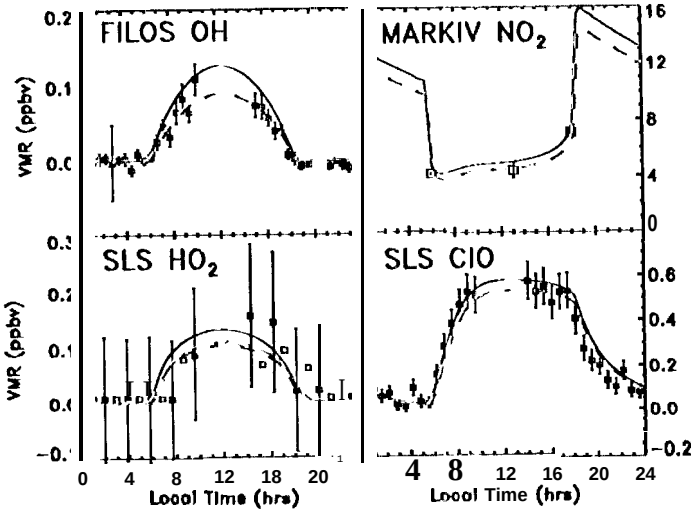
FILOS OH
MARKIV NO_2
SLS HO_2
SLS ClO
VMR (ppbv)
VMR (ppbv)
Local Time (hrs)
Local Time (hrs)
0.2
0.1
0.0
16
12
8
4
0
0.6
0.4
0.2
0.0
−0.2
0
4
8
12
18
20
4
8
12
16
20
24

Figure 1

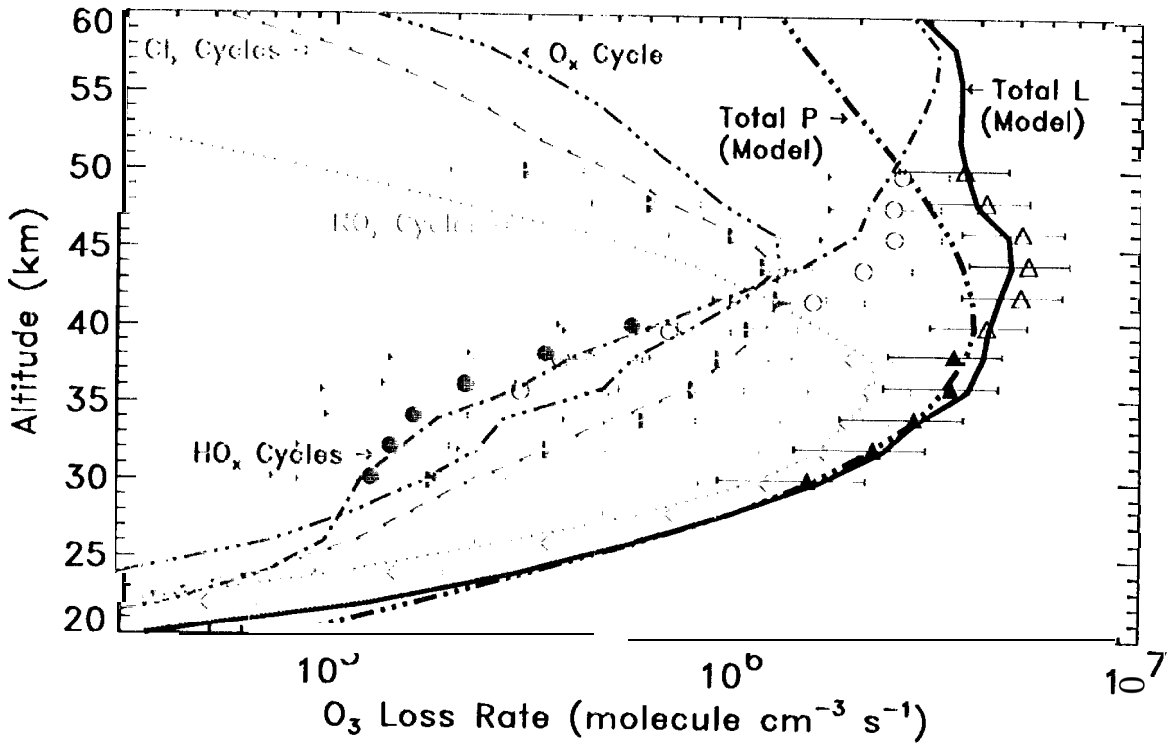
60
55
50
45
40
35
30
25
20
Altitude (km)
Cl$_x$ Cycles →
O$_x$ Cycle
Total P → (Model)
← Total L (Model)
HO$_x$ Cycles →
10^5
10^6
10^7
O$_3$ Loss Rate (molecule cm^{-3} s^{-1})

Figure 2

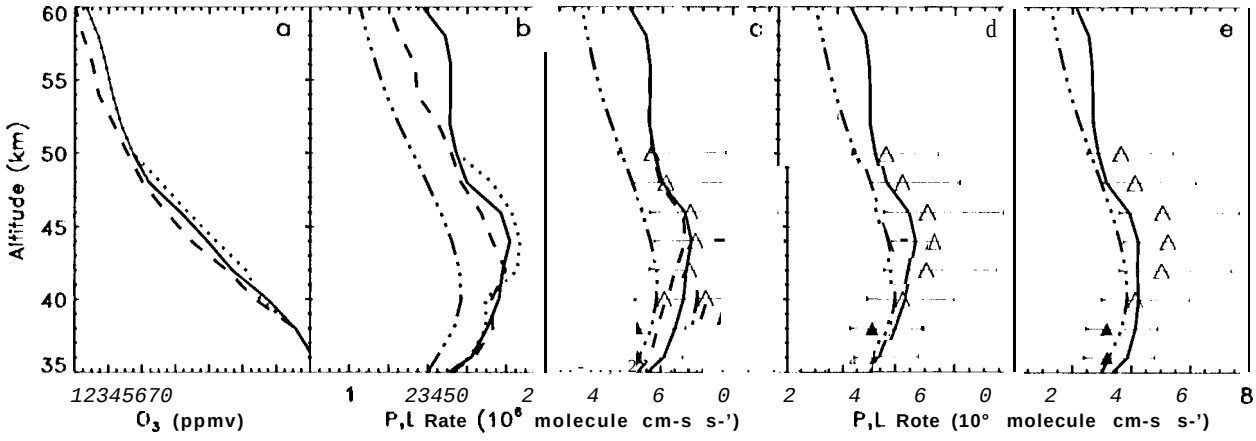
a
b
c
d
e
60
55
50
45
40
35
Altitude (km)
12345670
O3 (ppmv)
1 23450 2
P,L Rate (10^6 molecule cm-s s-')
4 6 0
2 4 6 0
P,L Rote (10° molecule cm-s s-')
2 4 6 8

Figure 3